

# Palmitate and glucose increase amyloid precursor protein in extracellular vesicles: Missing link between metabolic syndrome and Alzheimer's disease

Bhumsoo Kim<sup>1,2</sup>  | Yoon-Tae Kang<sup>3</sup> | Faye E. Mendelson<sup>1,2</sup> | John M. Hayes<sup>1,2</sup> | Masha G. Savelieff<sup>2</sup> | Sunitha Nagrath<sup>3</sup> | Eva L. Feldman<sup>1,2</sup>

<sup>1</sup>Department of Neurology, University of Michigan, Ann Arbor, Michigan, USA

<sup>2</sup>NeuroNetwork for Emerging Therapies, University of Michigan, Ann Arbor, Michigan, USA

<sup>3</sup>Department of Chemical Engineering and Biointerfaces Institute, University of Michigan, Ann Arbor, Michigan, USA

## Correspondence

Eva L. Feldman, Department of Neurology, University of Michigan, Ann Arbor, MI 48109, USA.

Email: [efeldman@umich.edu](mailto:efeldman@umich.edu)

## Funding information

Sinai Medical Staff Foundation; National Institutes of Health, Grant/Award Numbers: R01DK130913, U24DK115255; A. Alfred Taubman Medical Research Institute; NeuroNetwork for Emerging Therapies; Andrea and Lawrence A. Wolfe Brain Health Initiative Fund; Robert E. Nederlander Sr. Program for Alzheimer's Research; Michigan Diabetes Research Center for the confocal imaging to Michigan Diabetes Research Center for the confocal imaging, Grant/Award Number: P30DK02572

## Abstract

The metabolic syndrome (MetS) and Alzheimer's disease share several pathological features, including insulin resistance, abnormal protein processing, mitochondrial dysfunction and elevated inflammation and oxidative stress. The MetS constitutes elevated fasting glucose, obesity, dyslipidaemia and hypertension and increases the risk of developing Alzheimer's disease, but the precise mechanism remains elusive. Insulin resistance, which develops from a diet rich in sugars and saturated fatty acids, such as palmitate, is shared by the MetS and Alzheimer's disease. Extracellular vesicles (EVs) are also a point of convergence, with altered dynamics in both the MetS and Alzheimer's disease. However, the role of palmitate- and glucose-induced insulin resistance in the brain and its potential link through EVs to Alzheimer's disease is unknown. We demonstrate that palmitate and high glucose induce insulin resistance and amyloid precursor protein phosphorylation in primary rat embryonic cortical neurons and human cortical stem cells. Palmitate also triggers insulin resistance in oligodendrocytes, the supportive glia of the brain. Palmitate and glucose enhance amyloid precursor protein secretion from cortical neurons via EVs, which induce tau phosphorylation when added to naïve neurons. Additionally, EVs from palmitate-treated oligodendrocytes enhance insulin resistance in recipient neurons. Overall, our findings suggest a novel theory underlying the increased risk of Alzheimer's disease in MetS mediated by EVs, which spread Alzheimer's pathology and insulin resistance.

## KEYWORDS

Alzheimer's disease, amyloid precursor protein, diabetes, extracellular vesicles, insulin resistance, metabolic syndrome, obesity, tau

## 1 | INTRODUCTION

Metabolic syndrome (MetS) and Alzheimer's disease share several pathological features. Both are age-related processes characterised by insulin resistance, metabolic and mitochondrial dysfunction (Kim & Feldman, 2012; Neth & Craft, 2017; O'Neill & O'Driscoll, 2015), vascular deficits (Di Grandl & Wolfrum, 2018; Marco et al., 2015), chronic inflammation and oxidative stress (Van Dyken & Lacoste, 2018; Verdile et al., 2015) and abnormal protein processing (Gerakis & Hetz, 2018; Mohan et al., 2019). MetS is characterised by a constellation of metabolic dysfunctions, including elevated fasting glucose (prediabetes, type 2 diabetes), obesity, dyslipidaemia and hypertension (Grundy et al., 2005), which is aggravated by a diet rich in sugars and saturated

This is an open access article under the terms of the [Creative Commons Attribution-NonCommercial-NoDerivs License](https://creativecommons.org/licenses/by-nc-nd/4.0/), which permits use and distribution in any medium, provided the original work is properly cited, the use is non-commercial and no modifications or adaptations are made.

© 2023 The Authors. *Journal of Extracellular Vesicles* published by Wiley Periodicals LLC on behalf of International Society for Extracellular Vesicles.

fatty acids, such as palmitate (O'Neill & O'Driscoll, 2015). Reinforcing similarities between MetS with Alzheimer's disease, several population studies show MetS and its components raise the risk of future Alzheimer's disease development (Pedditzi et al., 2016; Biessels & Despa, 2018; Power et al., 2018; Sadahiro et al., 2019).

Alzheimer's disease histopathology in the brain is most characteristically marked by extracellular amyloid beta ( $A\beta$ ) plaques and intracellular hyperphosphorylated and/or truncated tau aggregates (Savelieff et al., 2013).  $A\beta$  is derived from the amyloid precursor protein (APP) through amyloidogenic processing by  $\beta$ - and  $\gamma$ -secretase to generate predominantly 40- and 42-residue  $A\beta$  species (Savelieff et al., 2013; Andrew et al., 2016). Alternate APP processing by  $\alpha$ - and  $\gamma$ -secretase yields a non-amyloidogenic fragment. APP phosphorylation at threonine (Thr) 668 enhances amyloidogenic  $A\beta$  production (Lee et al., 2003; Vingtdoux et al., 2005) and blocking this site prevents memory and synaptic plasticity deficits in mice (Lombino et al., 2013). Insulin resistance increases Thr668 APP phosphorylation in rat embryonic cortical neurons (eCNs) and mouse brain (Kim et al., 2019) and affects tau phosphorylation and truncation (Kim et al., 2009; Kim et al., 2013; Kim et al., 2015). Excess sugars and palmitate from Western-style diets induce insulin resistance and MetS (Palomer et al., 2018; Rumora et al., 2019). In Alzheimer's disease, hyperglycaemia (Takeda et al., 2010) and excess dietary palmitate aggravates pathology in mouse models (Busquets et al., 2017; Marwarha et al., 2019; Rollins et al., 2019). Overall, these findings demonstrate a link between brain insulin resistance (Kim & Feldman, 2012) and MetS with  $A\beta$  pathology, which raises the risk of cognitive decline and Alzheimer's disease (Sims-Robinson et al., 2010; Kim & Feldman, 2015; Matioli & Nitrini, 2015).

Despite molecular and epidemiological links, how MetS leads to Alzheimer's disease is not fully understood. Extracellular vesicles (EVs) are of particular interest as a point of convergence between MetS and Alzheimer's disease. EVs are cell-derived membranous structures that vary in size and origin, that is, endosomal or from plasma membrane shedding (van Niel et al., 2018). They carry cargo ranging from RNAs, protein and metabolites, and are linked, through intercellular communication, to numerous illnesses. EVs are implicated in MetS (Martinez & Andriantsitohaina, 2017; Pardo et al., 2018) and Alzheimer's disease (Xiao et al., 2017; DeLeo & Ikezu, 2018). MetS alters cargo composition and production of extracellular vesicles (Eguchi et al., 2016; Freeman et al., 2018). In Alzheimer's disease, cortical neurons release EVs that contain endogenous  $A\beta$  (Sardar Sinha et al., 2018), APP (Laulagnier et al., 2018) and tau (Wang et al., 2017), which transmit to recipient neurons to spread pathology.

Palmitate exposure of microglia, the immune glia of the brain, produces EVs that adversely affect neurons' ability to form dendritic spines (Vinueza et al., 2019), which could impact cognition, and emphasises the importance of neuron-glia interactions through EVs. Moreover, patients with Alzheimer's disease have circulating EVs that harbour biomarkers of brain insulin resistance (Mullins et al., 2017). However, the role of palmitate- and high glucose-induced insulin resistance in the brain as it pertains to its potential link to EVs in Alzheimer's disease remains unknown.

Herein, to clarify a possible role, we treated primary rat embryonic cortical neurons and human cortical stem cells with palmitate or glucose and found they developed insulin resistance and enhanced APP phosphorylation. Palmitate also induced insulin resistance in oligodendrocytes, the myelin glia of the brain. EVs isolated from palmitate- or glucose-treated neurons contained higher APP levels, and could transmit Alzheimer's disease pathology when added to recipient cells by raising phosphorylated tau (ptau). EVs derived from palmitate treated oligodendrocytes induced insulin resistance in recipient neurons. Overall, our findings suggest that elevated glucose and saturated fatty acids, such as palmitate, precipitate amyloid pathology in neuronal cell models and could provide the missing link between MetS with increased Alzheimer's disease risk.

## 2 | MATERIALS AND METHODS

### 2.1 | Antibodies and chemicals

All antibodies used are listed in Table S1. Horseradish peroxidase-conjugated secondary antibodies against rabbit (catalog # 7074, RRID:AB\_2099233) and mouse (catalog # 7076, RRID:AB\_330924) were from Cell Signalling Technology (Danvers, MA). Palmitate (catalog # P9767) and oleate (catalog # O7501) were from MilliporeSigma (St Louis, MO). Fatty acid-free bovine serum albumin (BSA) was from Thermo Fisher Scientific (catalog # BP9704, Waltham, MA).

### 2.2 | Cell culture and treatments

Human HK-532 cortical stem cells (Johe et al., 1996) were provided by Palisade Bio (Carlsbad, CA) under a Materials Transfer Agreement. The cells were differentiated in differentiation media (NSDM; DMEM with 100  $\mu$ M putrescine, 20 nM progesterone, 30 nM Na-selenite, 2  $\mu$ g/mL L-alanine, 0.83  $\mu$ g/mL L-asparagine, 7.7  $\mu$ g/mL L-proline, 0.34  $\mu$ g/mL vitamin B12, 100  $\mu$ g/mL apotransferrin, 25  $\mu$ g/mL insulin) for 7–10 days (Figure S1). Cell media was changed to insulin-free NSDM before fatty acid or glucose treatment (Kim et al., 2015). NSDM media is serum free, and all HK-532 experimentation was performed serum free. Pregnant Sprague Dawley rats were euthanised per our published protocols by sodium pentobarbital overdose (Vincent et al., 2005) and primary eCNs were prepared from E15 embryos. Primary rat eCNs were prepared from E15 embryos from

Sprague Dawley rats euthanised per our published protocols by sodium pentobarbital overdose (Vincent et al., 2005). eCNs were maintained in feed media [Neurobasal (catalog # 21103-049, GIBCO, Thermo Fisher Scientific) supplemented with B27 (catalog # 17504-044, GIBCO, Thermo Fisher Scientific) and other supplements as described (Kim et al., 2013)]. After 7 days, the culture media was changed to B27-free feed media prior to fatty acid or glucose treatment. eCN media is serum free, and all eCN experimentation was performed serum free. Human oligodendrocytes were from MilliporeSigma (catalog # SCC163) and maintained in DMEM (GIBCO, Thermo Fisher Scientific) with 10% heat-inactivated fetal bovine serum (catalog # F4135) (Figure S2). HOG cultures were serum starved for at least 4 h prior to experimentation, which was performed under serum free conditions. eCN, HK-532 and oligodendrocyte cultures were treated with fatty acids dissolved in boiling water and conjugated to fatty acid-free BSA for 1 h before cell treatment at the final concentrations indicated in each experiment (Rumora et al., 2018). Control cultures were treated with same volume of fatty acid-free BSA.

### 2.3 | EV isolation and treatment of naïve recipient neurons

EVs were isolated from cell culture media using Total Exosome Isolation Reagent (TEIR, catalog # 4478359, Invitrogen, Thermo Fisher Scientific) as previously described (Helwa et al., 2017), followed by ultracentrifugation. Briefly, cell culture supernatants were sequentially centrifuged at 300 g for 10 min, 2000 g for 10 min and 10,000 g for 30 min. The supernatant was filtered through 0.45  $\mu$ M syringe filter, incubated with 0.5 volume of the TEIR reagent overnight at 4°C, and centrifuged at 10,000 g for 1 h. The resulting pellets were dissolved in PBS and further ultracentrifuged for 3 h at 100,000 g at 4°C. The final EV pellets were dissolved in SDS-PAGE sample buffer for Western immunoblotting (see Section 2.6) or in culture media (B27- and insulin-free feed media for eCNs, insulin-free NSDM for HK-532 neurons) and added to naïve recipient neurons for 24 h, which were analysed by Western immunoblotting.

### 2.4 | Nanoparticle tracking analysis (NTA)

NTA was used to evaluate the concentration and the size distribution of the isolated vesicles using the NanoSight NS 300 (Marvern Instruments, UK). The NS 300 visualises the light scattered by the particles of interest based on the Brownian motion of nanoparticles to profile concentrations and size distributions. For each measurement, 30  $\mu$ L of the prepared solution was used and the movement was monitored for 20 s in triplicate. All data were acquired and processed using NanoSight NS 300 control software. For comparing samples, only the number and concentration of EVs, ranging 30–150 nm, were evaluated.

### 2.5 | Dil-labelling of EVs

EVs were purified as above from supernatant from HK-532 cultures using TEIR and ultracentrifugation. EVs were labelled with DiI dye (catalog # V22885, Invitrogen) as described (Chen et al., 2020). Briefly, 100  $\mu$ g of EVs (assayed by Pierce 660 Protein Assay Reagent) were dissolved in 200  $\mu$ L media and mixed with 0.5  $\mu$ L DiI in 100  $\mu$ L PBS for 30 min at 37°C. To remove excess DiI, 10 mL of cold PBS was added to the mixture and centrifuged at 100,000 g for 3 h at 4°C. The resulting DiI-labelled EVs were added to recipient HK-532 cells on cover slips for 24 h. Supernatant from the ultracentrifugation was used as the control and processed with the same amount of DiI along with the EV fraction. HK-532 cells were fixed with 4% paraformaldehyde and mounted on glass slides with ProLong gold with DAPI (Invitrogen, catalog # P36931). Images were taken on the Leica Stellaris 8 Lightning confocal using a 1.4 numerical aperture Plan-APO 63x oil objective. Images were rendered with the lightning deconvolution feature and were exported as tiffs (Elzinga et al., 2022).

### 2.6 | Western immunoblotting (WB)

WB was performed as previously (Kim et al., 2015). Cultured cells were lysed in RIPA buffer (catalog # 8990, Pierce, Thermo Fisher Scientific) containing protease inhibitor cocktail (catalog # 11836170001, Roche Diagnostics, Indianapolis, IN). Lysates were briefly sonicated and centrifuged for 20 min at 13,000 rpm at 4°C. Supernatants were collected and protein concentrations were measured with the Pierce 660 Protein Assay Reagent (catalog # 22660, Thermo Fisher Scientific), and the same amount of the lysate proteins were resolved by SDS-PAGE. Isolated EVs were dissolved in SDS-PAGE sample buffer, and protein concentrations were measured. Equal amounts of EV sample protein were loaded into wells, which were resolved by SDS-PAGE. Resultant gels (from cell lysates or EVs) were transferred to nitrocellulose membranes, which were blocked with 3% BSA in TBS with 0.1% Tween-20. Nitrocellulose membranes were next incubated with primary antibody overnight at 4°C, rinsed, and incubated for 2 h at room temperature with the appropriate horseradish peroxidase-conjugated secondary antibody. Bands were visualised

using Clarity Western ECL (catalog # 1705061, BioRad, Hercules, CA) or Calrity Max Western ECL (catalog # 1705062, BioRad), depending on the signal strength. Images were captured using the ChemiDoc Imaging System and analysed by Image Lab software (Bio-Rad). In some experiments analysing phospho-protein and total protein, blots were first probed for the phospho-protein and then the same nitrocellulose membranes were stripped for 15 min at 60°C in stripping solution (2% SDS, 100 mM dithiothreitol, 100 mM Tris, pH 6.8) and then probed with an additional antibody for total protein and actin or tubulin. All WB were repeated at least three times and representative results are shown in the figures.

## 2.7 | Statistical analysis

All experiments were repeated at least three times and presented as the mean  $\pm$  standard error of the mean. Statistical analysis was performed by Prism (GraphPad Software, San Diego, CA) by either one-way analysis of variance (ANOVA) with Tukey's post hoc or Student's *t*-test, depending on the number of comparison groups. Statistical significance was defined as  $p < 0.05$ .

## 3 | RESULTS

### 3.1 | Palmitate and glucose induce insulin resistance in vitro in neurons

Insulin receptor substrate 1 (IRS-1) phosphorylation stimulates its degradation and is a prominent insulin resistance mechanism (Coppes & White, 2012). C-jun N terminal kinases (JNKs), a mitogen-activated protein kinase subfamily, are also implicated in MetS and Alzheimer's disease, and induce insulin resistance by inhibiting insulin signalling (Yarza et al., 2015; Ono, 2019). Therefore, we first examined phosphorylation of IRS-1 (pIRS-1) and JNK (pJNK) as insulin resistance markers. Palmitate (150  $\mu$ M, 24 h) increased pIRS-1 (Ser612) and pJNK in rat primary embryonic cortical neurons (eCNs) (Figure 1a,b), indicating induction of insulin resistance. Palmitate similarly raised pIRS-1 (Ser612 and Ser636/639) and pJNK levels in differentiated human cortical stem cells (HK-532 neurons) (Figure 1c,d). Dyslipidemia is only one possible MetS component; thus, we also investigated the influence of elevated glucose, another MetS component, on neurons. Elevated glucose treatment (50 mM, 24 h) similarly enhanced pIRS-1 (Ser612) and pJNK levels in eCNs, indicative of insulin resistance induction (Figure 1e,f).

Akt phosphorylation (pAkt) mediates insulin's metabolic effects and plays critical roles in insulin resistance (Kim & Feldman, 2012). We previously demonstrated that short-term insulin treatment activates Akt, but chronic long-term insulin exposure leads to insulin resistance and blunts Akt activation in both central nervous system and peripheral neurons (Kim et al., 2015; Kim, McLean, et al. 2011; Kim, Sullivan, et al. 2011). Herein, as anticipated, 30 min of insulin treatment significantly increased pAkt in eCNs, without affecting total Akt, in the absence of palmitate (Figure 1g,h). Insulin still activated Akt in palmitate pretreated eCNs, but the response was blunted, confirming palmitate-mediated insulin resistance. Insulin also induced extracellular signal-regulated kinase (ERK) phosphorylation (pERK) in eCNs (Figure 1g,h); however, ERK phosphorylation was not affected by palmitate treatment, indicating the specificity of palmitate only to Akt signalling. These observations were also replicated in human HK-532 neurons, with palmitate-induced blunting of insulin signalling (Figure 1i,j), indicating generalisability of these findings.

In contrast to the saturated fatty acid palmitate, the monounsaturated fatty acid, oleate, did not induce insulin resistance in cortical neurons. We treated HK-532 neurons with oleate (150  $\mu$ M, 48 h) versus palmitate (150  $\mu$ M, 48 h) versus control conditions (bovine serum albumin vehicle) and stimulated with insulin (Figure 1k,l). Akt was phosphorylated to the same extent in control- and oleate-treated neurons. However, Akt phosphorylation was blunted in palmitate-treated neurons, with significantly lower pAkt levels versus control and oleate samples, indicative of insulin resistance in palmitate samples. Insulin stimulation also phosphorylated ERK, but the extent of activation did not differ among the three conditions, oleate, palmitate and control (Figure 1k,l), suggesting insulin resistance occurred specifically through Akt signalling. Thus, insulin resistance in neurons may develop from long-chain saturated but not monounsaturated fatty acids.

### 3.2 | Palmitate and glucose increase pAPP in vitro in neurons

In addition to the link with the MetS, insulin resistance is also a central aspect of Alzheimer's disease (Kellar & Craft, 2020). We previously showed that chronic insulin treatment triggers insulin resistance in neurons in tandem with enhanced APP phosphorylation (pAPP) at Thr668 (Thr668-pAPP) (Kim et al., 2019). This APP modification favours amyloidogenic processing and A $\beta$  production (Lee et al., 2003; Vingtdeux et al., 2005). Moreover, APP is a JNK substrate (Standen et al., 2001), which increases Thr668-pAPP levels in an okadaic acid-induced model of neuronal degeneration (Ahn et al., 2016), reinforcing the link between insulin resistance, through JNK activation, with the phosphorylation state of APP. Here, we examined the influence of MetS conditions on neuronal insulin resistance and Thr668-pAPP levels in both rat eCNs and HK-532 neurons. Palmitate



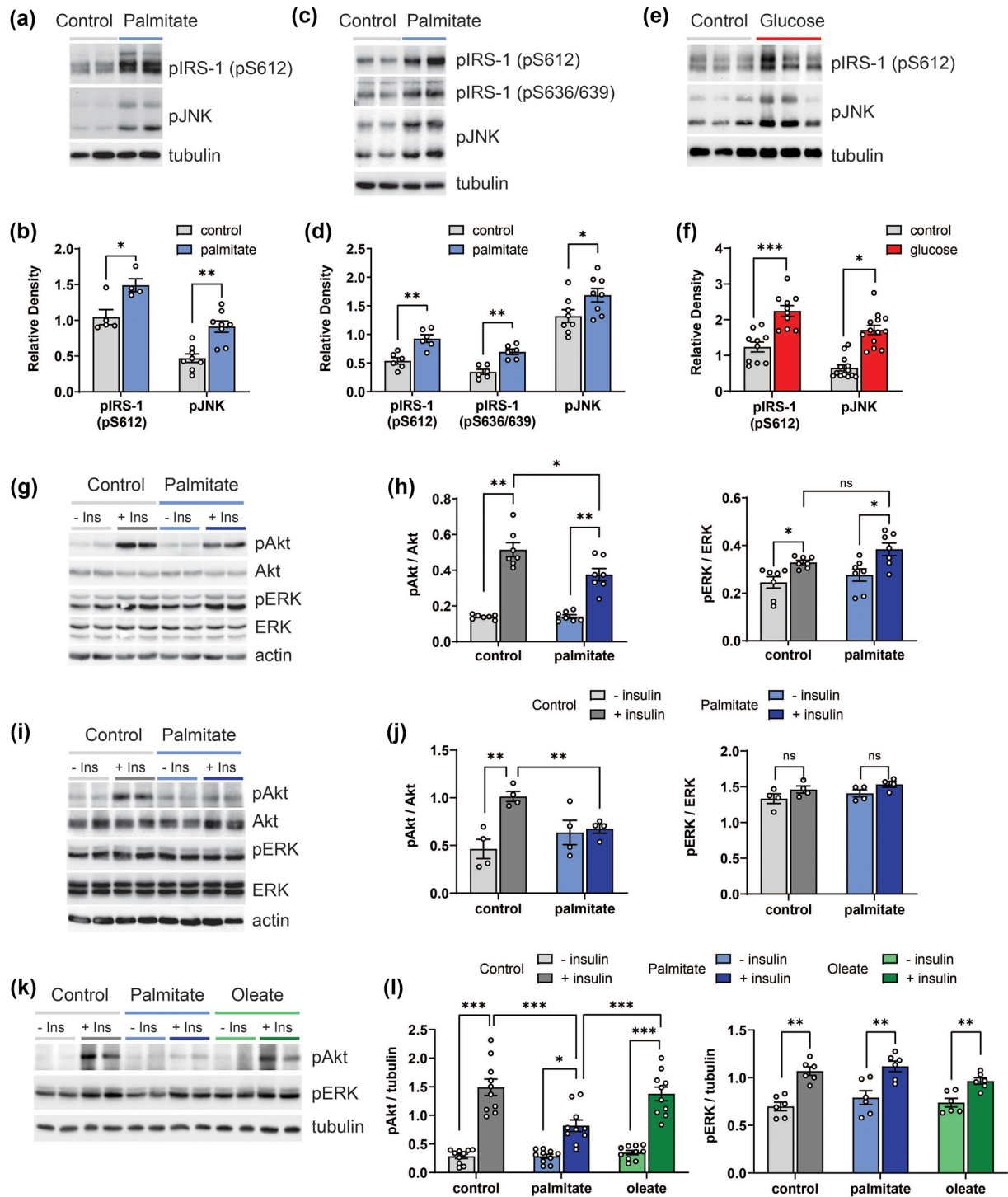


**FIGURE 1** Palmitate and glucose induce insulin resistance in vitro in neurons. (a, b) Rat eCNs or (c, d) differentiated human HK-532 cortical stem cells were treated with control (BSA) or palmitate (150  $\mu$ M) for 48 h and cell lysates were analysed by Western blotting (WB) for pIRS-1 (pS612) and pJNK. The same blots were stripped and re-probed for tubulin (loading control). Relative levels from WB analysis for pIRS-1 and pJNK in control- versus palmitate-treated neurons are represented in the graph (b, d). (e, f) eCNs were treated with control (media) or glucose (50 mM) for 24 h and cell lysates were analysed by WB for pIRS-1 and pJNK. The same blots were stripped and re-probed for tubulin (loading control). Relative levels from WB analysis for pIRS-1 and pJNK in control- versus glucose-treated neurons are represented in the graph (f). (g) eCNs were treated with control (BSA) or palmitate (150  $\mu$ M) for 48 h followed with/without insulin (20 nM) for 30 min and cell lysates were analysed by WB for pAkt and pERK. The same blots were stripped and re-probed for total Akt and ERK, and actin. (h) Relative levels from WB analysis of pAkt versus total Akt and pERK versus total ERK are represented in the graph. (i) HK-532 neurons were treated with control (BSA) or palmitate (150  $\mu$ M) for 48 h followed with/without insulin (20 nM) for 30 min and cell lysates were analysed by WB for pAkt and pERK. The same blots were stripped and re-probed for total Akt and ERK, and actin. (j) Relative levels from WB analysis of pAkt versus total Akt and pERK versus total ERK in HK-532 neurons with/without acute insulin are represented in the graph. (k) HK-532 neurons were treated with control (BSA) or oleate (150  $\mu$ M) or palmitate (150  $\mu$ M) for 48 h followed with/without insulin (20 nM) for 30 min and cell lysates were analysed by WB for pAkt and pERK. The same blots were stripped and re-probed for total Akt and ERK, and tubulin. (l) Relative levels from WB analysis of pAkt versus tubulin and pERK versus tubulin in HK-532

(Continues)

FIGURE 1 (Continued)

neurons with/without acute insulin are represented in the graph. Data are presented as mean  $\pm$  standard error of the mean (SEM) from at least 3 separate experiments. \* $p < 0.05$ , \*\* $p < 0.01$ , by Student's  $t$ -test; ns, no statistical difference.

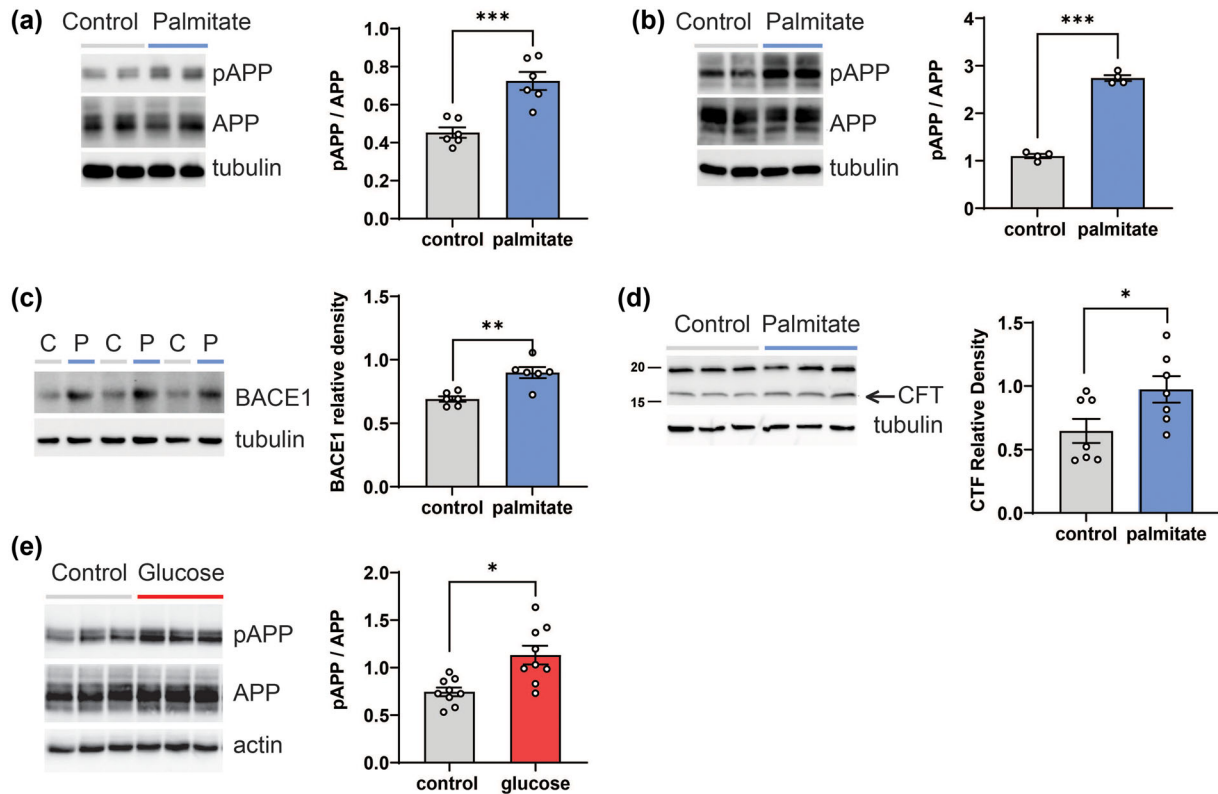


**FIGURE 2** Palmitate and glucose increase pAPP in vitro in neurons. (a) Rat eCNs or (b) differentiated human HK-532 cortical stem cells were treated with control (BSA) or palmitate (150  $\mu$ M) for 48 h and cell lysates were analysed by WB (left panels) for pAPP. The same blots were stripped and re-probed for total APP and tubulin. Right panels: Relative levels from WB analysis of pAPP versus total APP in control- versus palmitate-treated neurons. (c) HK-532 neurons were treated with control (C, BSA) or palmitate (P, 150  $\mu$ M) for 48 h and cell lysates were analysed by WB (left panel) for BACE1. Relative levels from WB analysis of BACE1 is shown in the right panel. (d) HK-532 cells were treated as in (c) and CTF levels were analysed. (e) Rat eCNs were treated with control (media) or glucose (50 mM) for 24 h and cell lysates were analysed by WB for pAPP. The same blots were stripped and re-probed for total APP and actin. Data are presented as mean  $\pm$  SEM from at least three separate experiments. \* $p < 0.05$ , \*\*\* $p < 0.001$ , by Student's  $t$ -test.

treatment increased Thr668-pAPP, without affecting net APP levels, in both eCNs (Figure 2a) and HK-532 neurons (Figure 2b). Palmitate-treated HK-532 neurons also had amplified expression of  $\beta$ -secretase 1 (BACE1) (Figure 2c), a secretase that enhances APP cleavage predominantly into amyloidogenic A $\beta$ -40 and A $\beta$ -42 species (Savelieff et al., 2013). APP processing by BACE1 also produces C-terminal fragment (CTF), which is considered as the precursor of A $\beta$  generation (Miranda et al., 2018; Perez-Gonzalez et al., 2020). We found CTF levels increased along with BACE1 after palmitate treatment (Figure 2d). Palmitate-induced increased pAPP, BACE1 and CTF expression suggest activation of the amyloidogenic cleavage pathway. Treating eCNs with hyperglycaemic conditions similarly augments Thr668-pAPP levels relative to normoglycaemic conditions (Figure 2e). Overall, these results demonstrate the important role of insulin resistance on amyloidogenic processing and suggest a possible link between diabetes and Alzheimer's disease.

### 3.3 | Palmitate induces insulin resistance in vitro in oligodendrocytes

Brain metabolism occurs non-cell autonomously and involves glia, including oligodendrocytes, astrocytes and microglia, which metabolically coordinate with and support neurons (Henn et al., 2022). The development of insulin resistance in various cellular brain compartments, such as the neurons and glia, has implications for disease (Chen et al., 2022). However, relatively little is known about the development insulin resistance of oligodendrocytes, which, as the glia in direct contact with neurons, contribute substantially to neuronal metabolism and health (Henn et al., 2022). Therefore, we also assessed the impact of palmitate (150  $\mu$ M, 48 h) on human oligodendrocytes followed by insulin challenge (Figure 3a). Although palmitate-treated oligodendrocytes still

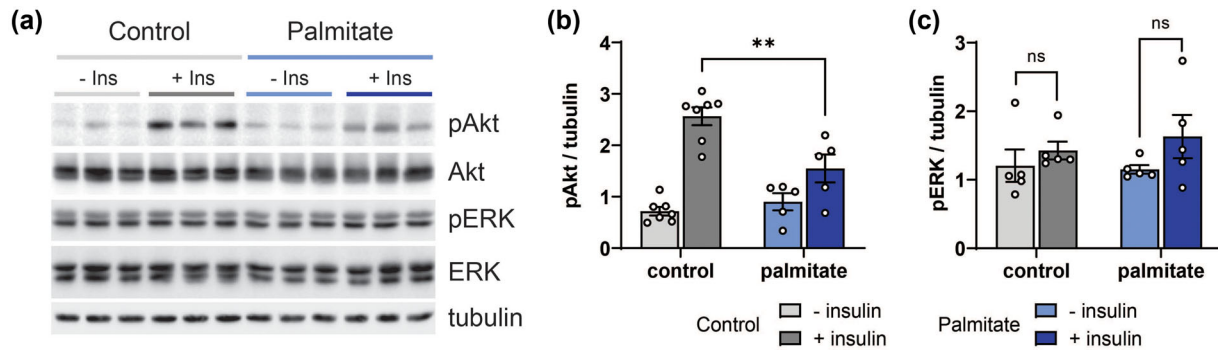


**FIGURE 3** Palmitate induces insulin resistance in vitro in oligodendrocytes. (a) Human oligodendrocytes were treated with control (BSA) or palmitate (150  $\mu$ M) for 48 h followed with/without insulin (20 nM) for 30 min and cell lysates were analysed by WB for pAkt and pERK. The same blots were stripped and re-probed for total Akt and ERK, and tubulin. Relative levels from WB analysis of (b) pAkt versus total Akt and (c) pERK versus ERK in control- versus palmitate-treated oligodendrocytes. Data are presented as mean  $\pm$  SEM from at least three separate experiments. \*\* $p$  < 0.01, by Student's  $t$ -test.

responded to insulin, as verified by some Akt activation (increased pAkt), the response was blunted compared to control-treated cultures (Figure 3b). The ERK pathway was not activated (Figure 3c), indicating specifically palmitate-mediated insulin resistance in oligodendrocytes.

### 3.4 | Palmitate enhances EV secretion in vitro from cortical neurons and oligodendrocytes

EV secretion is altered in the MetS (Martinez & Andriantsitohaina, 2017; Pardo et al., 2018) and in Alzheimer's disease (Xiao et al., 2017; DeLeo & Ikezu, 2018), suggesting a common point across these diseases. Thus, we were interested in EV dynamics in our palmitate-induced insulin resistance models of neurons and oligodendrocytes. We isolated EVs through a process outlined in Section 2. We first assessed our EV preparation from HK-532 neurons (Figure 4a) and oligodendrocytes (Figure 4b) using well-established markers, tumour susceptibility gene 101 (TSG101) (Kowal et al., 2016), flotillin and Alix (Laulagnier et al., 2018). Meanwhile, endoplasmic reticulum (calnexin) or mitochondrial (voltage-dependent anion channel, VDAC) proteins were absent from the preparation, suggesting it was mainly comprised of EVs (Vella et al., 2017; They et al., 2018). We further analysed our EV isolations by NTA, which showed similar profiles in two samples (Figure 4c, panels i–ii). NTA found the two samples were of similar concentration (sample 1,  $2.84 \times 10^9 \pm 2.69 \times 10^8$ , sample 2,  $2.29 \times 10^9 \pm 4.95 \times 10^7$  EV/mL), and of similar size distributions, with most ranging from 30 to 150 nm (sample 1,  $66.58 \pm 0.09\%$ , sample 2,  $65.76 \pm 1.45\%$ ; Figure 4c, panels iii–iv). Thus, our EV isolation was consistent and reproducible and contained mostly small EVs 30 to 150 nm in size. Next, we treated HK-532 neurons (Figure 4d) and oligodendrocytes (Figure 4e) with palmitate (150  $\mu$ M, 48 h) versus control conditions and isolated EVs. In both instances, palmitate stimulated EV secretion from neurons and oligodendrocytes (Figure S3).

### 3.5 | Palmitate and glucose increase EV APP secretion in vitro from cells, and transmit tau pathology to recipient neurons

EVs carry various cargo, such as full length APP, A $\beta$ , and tau peptides, in Alzheimer's disease models (Xiao et al., 2017; DeLeo & Ikezu, 2018) and may contribute to disease spread by EV transmission to naïve recipient cells (Wang et al., 2017; Laulagnier et al., 2018; Sardar Sinha et al., 2018). Since palmitate and glucose enhanced pAPP in insulin resistant neurons (Figure 2), we next sought to determine whether MetS conditions increased APP cargo in secreted EVs, and whether these EVs were transmissible to naïve recipient cells. First, we examined the influence of MetS on EV APP cargo. We found that palmitate dose-dependently increased APP levels in EVs secreted from HK-532 cultures (Figure 5a,b). In contrast, the monounsaturated fatty acid oleate, which does not induce insulin resistance (Palomer et al., 2018), did not enhance APP EV levels relative to palmitate. Palmitate treatment also increased EV CTF level (Figure 5c,d), consistent with the results from lysate (Figure 2d). We also examined the impact of elevated glucose conditions, which similarly augmented EV APP cargo (Figure 5e,f). Palmitate and glucose treatment did not affect the cellular APP levels (Figure 2). Overall, this indicates that APP-loaded EV secretion may be related to induction of insulin resistance.

Next, we tested the transmissibility of EVs isolated from HK-532 cells by labelling with DiI dye and adding them to naïve recipient cells. Confocal images show a punctate pattern of DiI-labelled EV internalised by recipient cells (Figure 6Ab & Ac), while DiI conjugated with supernatant after ultracentrifugation show no signal (Figure 6Aa). We next examined whether EVs from palmitate- or glucose-treated cells transmit Alzheimer's disease pathology, namely tau phosphorylation

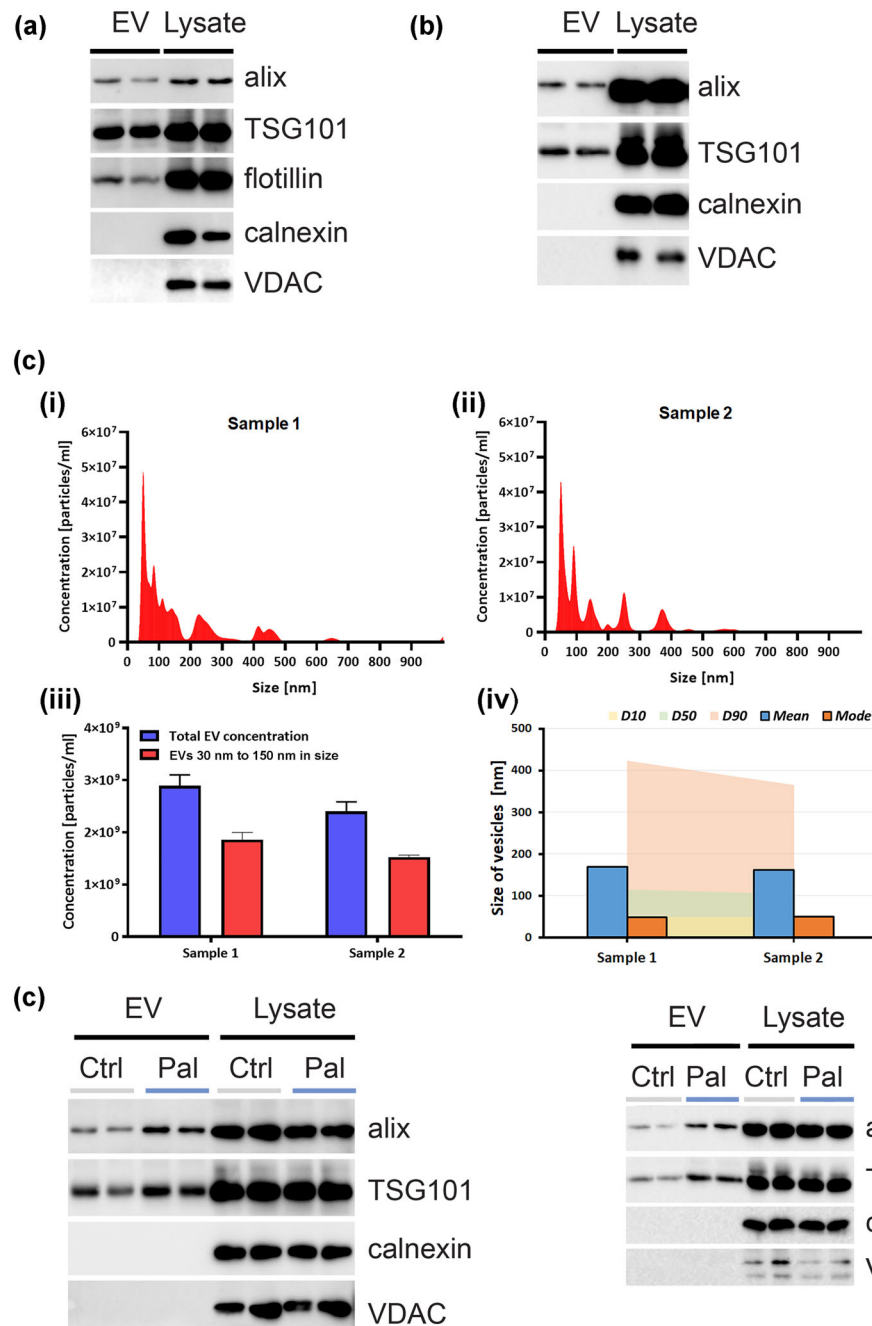


**FIGURE 4** Palmitate enhances EV secretion in vitro from cortical neurons and oligodendrocytes. EVs were purified from control (BSA-treated) (a) HK-532 neurons or (b) oligodendrocyte culture supernatant by ultracentrifugation. EVs and lysate were analysed by WB for TSG101, flotillin and Alix (EV biomarkers) and calnexin, VDAC or argonaute (cellular biomarkers). (c-i & c-ii) Nanoparticle tracking analysis profiles of EVs from two different isolations (sample 1 & sample 2). (c-iii) Concentration of EVs (30–150 nm) and (c-iv) Particle size distribution analysis of vesicles from two different isolations. EVs were purified from control (Ctrl)- or palmitate (Pal, 150  $\mu$ M, 48 h)-treated (d) HK-532 neurons or (e) oligodendrocyte culture supernatant, and EV and cellular markers were analysed.

(Savelieff et al., 2013). To examine whether MetS conditions stimulate release of EVs that can spread Alzheimer's disease pathology, we purified EVs from control- and palmitate-treated HK-532 neuron culture supernatant and treated them to naïve recipient HK-532 cells. We found that tau phosphorylation increased at multiple residues in recipient neurons treated with EVs derived from palmitate- versus control-treated cells (Figure 6b,c). In a parallel vein, we isolated secreted EVs from supernatant from eCN cultures treated with high glucose versus control conditions. Again, tau phosphorylation was enhanced at multiple residues in naïve recipient neurons after treatment with high glucose- versus control-derived EVs (Figure 6d,e).

Cognitive impairment secondary to the MetS (Henn et al., 2022) and dementia in Alzheimer's disease (Vanzulli, Papanikolaou et al., 2020) occur non-cell autonomously, including through dysfunctional oligodendrocyte-neuron interactions



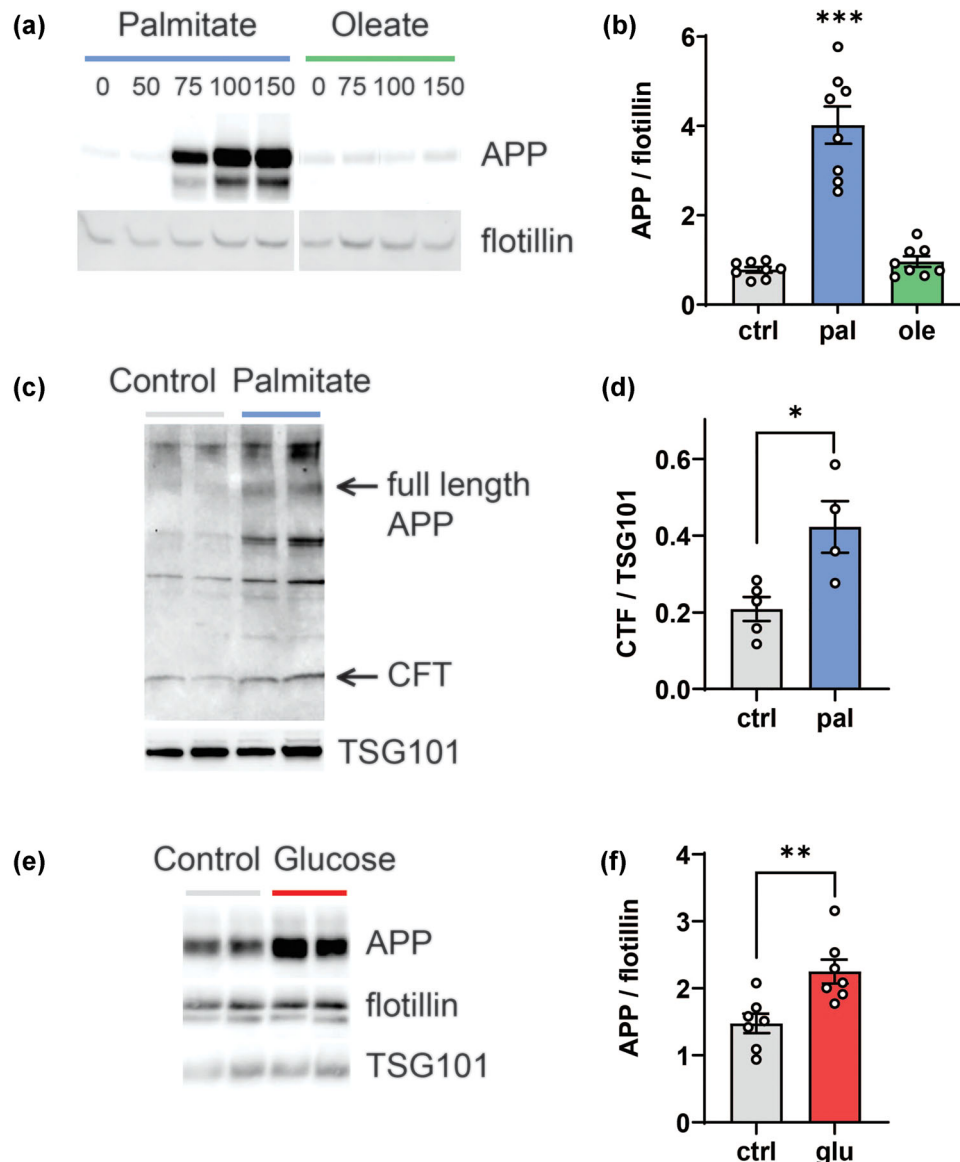


**FIGURE 5** Palmitate and glucose increase EV APP secretion in vitro from cells. (a) Differentiated human HK-532 cortical stem cells were treated with increasing palmitate or oleate concentrations (0 [BSA vehicle], 50, 75, 100 and 150  $\mu$ M) for 48 h. EVs were purified from culture supernatant and analysed by WB for APP and flotillin. (b) Relative levels from WB analysis for APP versus flotillin in 0 or 150  $\mu$ M palmitate or oleate represented in the graph. (c) HK-532 cells were treated with BSA (control) or 150  $\mu$ M palmitate for 48 h. EVs were purified from culture supernatant and analysed by WB for CTF (C-terminal fragment). (d) Relative levels from WB analysis for CTF versus TSG-101 is represented in the graph. (e) eCNs were treated with control (media) or glucose (glu; 50 mM) for 24 h. EVs were purified from cell culture media by ultracentrifugation and analysed by WB for APP versus flotillin and TSG101 as EV markers. (f) Relative levels from WB analysis for EV APP versus flotillin are represented in the graph. Data are presented as mean  $\pm$  SEM from at least three separate experiments. \* $p < 0.05$ , \*\* $p < 0.01$ , \*\*\* $p < 0.001$ , by Student's *t*-test.

(Chen et al., 2021), which is related to insulin resistance (O'Grady et al., 2019). Therefore, finally, we also examined whether EVs derived from oligodendrocyte glia under MetS conditions induce insulin resistance in recipient neurons. Indeed, EVs from palmitate-treated oligodendrocytes induced insulin resistance in recipient neurons (Figure 6f,g). These results suggest that palmitate treatment affects EV cargo content in a cell type specific manner, which eventually regulate the pathology of recipient neurons.

## 4 | DISCUSSION

The MetS and Alzheimer's disease share multiple pathological processes, including insulin resistance. Their similarities are also supported by a large body of epidemiological evidence that individuals with the MetS are at elevated risk of developing Alzheimer's disease in later life (Campos-Pena et al., 2017; Biessels & Despa, 2018). Although several molecular links have been

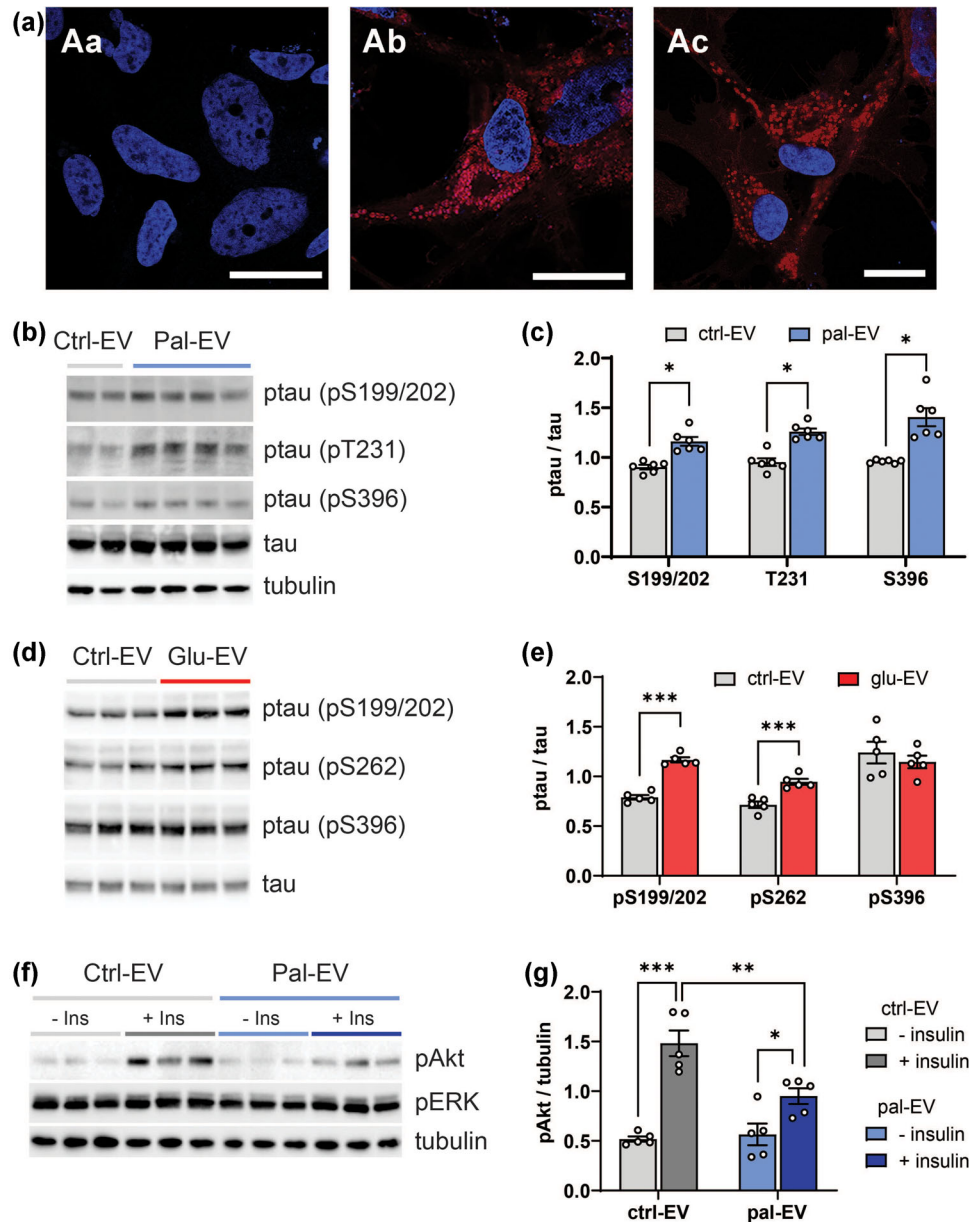


**FIGURE 6** EVs derived from palmitate- or glucose-treated cortical neurons and oligodendrocytes increase tau phosphorylation and induce insulin resistance, respectively, in recipient neurons in vitro. (a) EVs from HK-532 cells were labelled with Dil dye (red channel) and added to naïve recipient HK-532 cells for 24 h (Ab & Ac). Supernatant after ultracentrifugation was used as the no EV control (Aa). Blue channel, DAPI; scale bar = 20  $\mu$ m. (b) HK-532 neurons were treated with control (BSA) or palmitate (150  $\mu$ M) for 48 h. EVs were purified from control (Ctrl-EV) or palmitate (Pal-EV) culture supernatant by ultracentrifugation and added to naïve recipient HK-532 neurons for 24 h. Recipient HK-532 neuron lysates were analysed by WB for phosphorylated tau (ptau, pS199/202, pT231, pS396) and total tau. Equal protein loading was confirmed by tubulin. (c) Relative levels from WB analysis for ptau versus total tau in Ctrl-EV- versus Pal-EV-treated HK-532 neurons are represented in the graph. (d) EVs isolated from control (Ctrl-EV) or glucose (Glu-EV, 50 mM, 24 h) eCN culture supernatant were added to naïve recipient eCNs for 24 h and tau phosphorylation was analysed from the cell lysates. (e) Relative levels from WB analysis for ptau versus total tau in Ctrl-EV- versus Glu-EV-treated eCNs are represented in the graph. (f) Human oligodendrocytes were treated with control (BSA) or palmitate (150  $\mu$ M) for 48 h. EVs were purified from control (Ctrl-EV) or palmitate (Pal-EV) culture supernatant by ultracentrifugation and added to naïve recipient HK-532 neurons for 24 h. Recipient Ctrl-EV- or Pal-EV-treated HK-532 neurons were treated with 20 nM insulin for 30 min and lysates were analysed by WB for the indicated proteins. (g) Relative levels from WB analysis of pAkt in Ctrl-EV- versus Pal-EV-treated HK-532 are represented in the graph. Data are presented as mean  $\pm$  SEM from at least three separate experiments. \* $p$  < 0.05, \*\* $p$  < 0.01, \*\*\* $p$  < 0.001, by Student's *t*-test.

suggested, the precise mechanisms remain unknown. Herein we demonstrated that elevated palmitate and glucose induced insulin resistance and APP phosphorylation in neurons. Additionally, they enhanced APP and CTF secretion from cortical neurons via EVs, which can be transmitted to naïve neurons, where they triggered tau hyperphosphorylation, an Alzheimer's disease pathology. Thus, palmitate enhanced APP phosphorylation in cells and altered APP trafficking dynamics to vesicles. We also found that palmitate caused insulin resistance in oligodendrocytes, the supportive glia of the brain. These oligodendrocytes subsequently released EVs, which transmitted insulin resistance to naïve recipient neurons. Our data suggest a novel mechanism

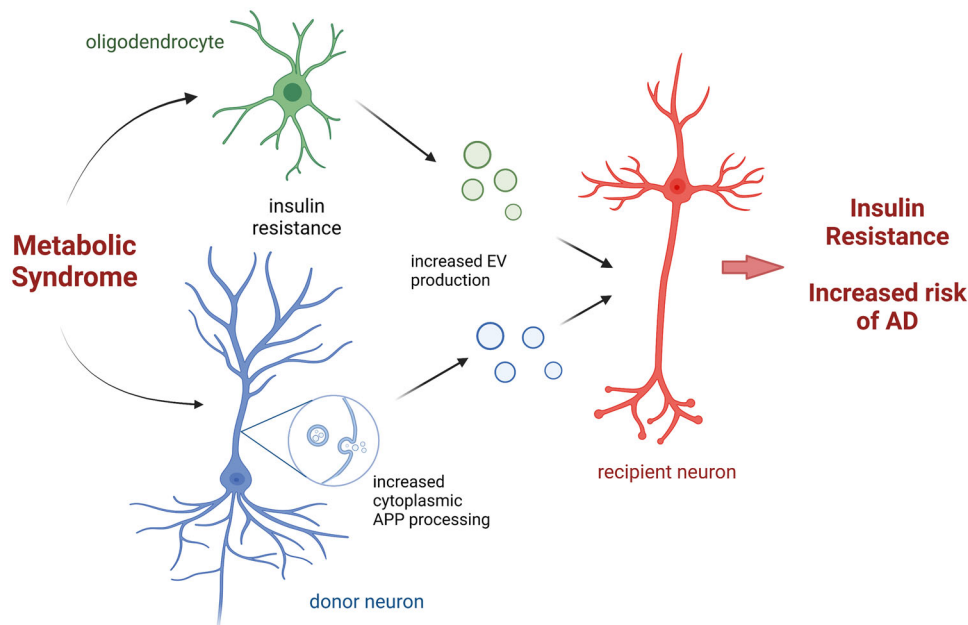


**FIGURE 7** Model figure. Metabolic syndrome induces insulin resistance in both neurons and oligodendrocytes. EVs secreted from these cells are taken up by nearby neurons, which further induces insulin resistance in recipient cells and increases risk of AD. Model is created with BioRender.com.

of insulin resistance and Alzheimer's pathology spread mediated by EVs, which underlies the predisposition of individuals with the MetS to Alzheimer's disease.

Insulin resistance is a recurrent theme across the MetS and Alzheimer's disease (Kim & Feldman, 2015; Neth & Craft, 2017). A Western-style diet rich in sugars and saturated fatty acids, such as palmitate, induces systemic insulin resistance and the MetS in people (Palomer et al., 2018). Moreover, the MetS may incur metabolic changes affecting the brain. Indeed, we have shown that neurons are insulin responsive and develop insulin resistance, even though they are not insulin-dependent (Kim, McLean, et al. 2011; Kim, Sullivan, et al. 2011; Kim & Feldman, 2012; Kim & Feldman, 2015; Kim et al., 2015). Likewise, the Alzheimer's disease brain is also characterised by insulin resistance and impaired glucose and fatty acid metabolism (Neth & Craft, 2017), including at various cellular compartments (Henn et al., 2022).

We previously illustrated a potential link between insulin resistances under MetS conditions to Alzheimer's disease pathology. We observed that acute insulin (2 h) decreases neuronal Thr668-pAPP (Kim et al., 2019), as reported by others (Pandini et al., 2013); however, chronic hyperinsulinemia (24 h), as occurring during insulin resistance, increases neuronal Thr668-pAPP levels (Kim et al., 2019), which would favour amyloidogenic APP processing (Ramelot & Nicholson, 2001; Matsushima et al., 2012; Pandini et al., 2013). Indeed, chronic insulin treatment does enhance extracellular A $\beta$  production (Gasparini et al., 2001; Pandini et al., 2013). We also found that hyperglycaemia- (Kim et al., 2009; Kim et al., 2013) and hyperlipidaemia-induced (Kim et al., 2015) insulin resistance triggers tau hyperphosphorylation and truncation, findings echoed by others (Kim, Park, et al. 2011). In this study, we now further show that elevated palmitate and glucose induce insulin resistance and increase neuronal APP phosphorylation at Thr668, which would enhance amyloidogenesis, as cited by other works (Patil et al., 2006; Marwarha et al., 2017). Therefore, we suggest that palmitate- and glucose-induced insulin resistance enhances Thr668-pAPP phosphorylation, which may explain the increased incidence of Alzheimer's disease and cognitive impairment among individuals with the MetS.

In addition to insulin resistance, altered EV dynamics are also shared features of the MetS (Martinez & Andriantsitohaina, 2017; Pardo et al., 2018) and Alzheimer's disease (Xiao et al., 2017; DeLeo & Ikezu, 2018). Thus, we next investigated the influence of dyslipidaemia and hyperglycaemia on EV APP. First, we verified that our purified EVs carried positive (Kowal et al., 2016; Laulagnier et al., 2018) and lacked negative (Vellaet al., 2017) biomarkers. We also confirmed that our purification method provided a reasonably consistent preparation of EVs, with most ranging from 30 to 150 nm in size by NTA analysis (Soo, Song et al., 2012). We found that elevated palmitate and glucose stimulated APP secretion from neurons via EVs. Our results agree with studies reporting palmitate-induced EVs from microglial (Vinuesa et al., 2019) and myoblast cultures and skeletal muscle in mice (Aswad et al., 2014). Obesity also significantly increases EV secretion from adipose tissue *in vivo*, contributing to tissue inflammation (Akbar et al., 2019).

In Alzheimer's disease, EVs are a well-established mechanism for disseminating pathology through pro-amyloidogenic cargo, including APP (Laulagnier et al., 2018), A $\beta$  (Sardar Sinha et al., 2018) and tau (Wang et al., 2017). Thus, we hypothesised EVs could constitute a spreading mechanism of insulin resistance-induced amyloid pathology in the MetS. Indeed, we demonstrated here for the first time that dyslipidaemia and hyperglycaemia conditions increased production from cortical neurons of EV bearing cargo,

that is, APP, CTF, that favours amyloid pathology. Importantly, we also showed that these high palmitate- and glucose-induced APP-containing EVs are transmissible and stimulated tau phosphorylation in recipient neurons. Unfortunately, we could not detect A $\beta$  in cell lysates or EVs by Western blotting or ELISA. However, we detected increased BACE1 and CTF in cell lysates and increased CTF in EVs. BACE1 is an enzyme essential for generating A $\beta$  (Savelieff et al., 2013) and CTF is the source of A $\beta$  following  $\gamma$ -secretase cleavage (Miranda et al., 2018; Perez-Gonzalez et al., 2020). Higher CTF in EVs was also reported in the brains of transgenic Tg2576 Alzheimer's disease mice, a model of human APP overexpression (Perez-Gonzalez et al., 2020). These results, albeit indirectly, suggest palmitate activates the amyloidogenic pathway. We speculate these increased amyloidogenic products in EVs are responsible for the increased tau phosphorylation in recipient cells.

Our findings suggest that the effect of elevated saturated fatty acids and glucose on APP-carrying EVs may be a point of convergence between the MetS and Alzheimer's disease and could possibly underlie the predisposition of individuals with the MetS to dementia (Figure 7) (Campos-Pena et al., 2017; Biessels & Despa, 2018). Yet, despite the importance to Alzheimer's disease pathology, the influence of EV secretion in the context of dysfunctional metabolism, that is, insulin resistance, dyslipidaemia, hyperglycaemia, has not been investigated to the best of our knowledge. However, the literature support various aspects regarding the impact of the MetS components on amyloid formation, palmitate aggravates APP and tau pathology in transgenic Alzheimer's disease mouse models (Barron et al., 2013; Marwarha et al., 2019), and even in wild-type animals, as we (Kim et al., 2015; Kim et al., 2019) and others (Busquets et al., 2017; Nakandakari et al., 2019) have shown. Hyperglycaemia similarly impairs tau dynamics in neuronal culture and diabetic mice (Kim et al., 2009; Kim et al., 2013; Kim et al., 2015) and diabetes worsens amyloid pathology and cognitive impairment in Alzheimer's disease mice (Takeda et al., 2010). Further, the literature supports that neuronally-derived EVs in Alzheimer's disease contain elevated ptau and A $\beta$ , which seed tau aggregation upon injection into the brain of healthy wild-type mice (Winston et al., 2016). Finally, neuronally-derived EVs from individuals with Alzheimer's disease harbour higher levels of insulin resistance biomarkers compared to healthy controls (Kapogiannis et al., 2015). Our study linked all these processes to suggest that elevated palmitate- and glucose-induced insulin resistance enhances EV secretion in the MetS, which may mediate Alzheimer's disease pathology (Figure 7).

We also found that induction of insulin resistance was specific to palmitate, since the monounsaturated fatty acid oleate, which is protective against the MetS (Palomer et al., 2018), did not affect insulin-induced Akt signalling. Furthermore, we found oleate only marginally enhanced EV APP shedding from neurons. The protective effect of oleate in neuronal cultures versus palmitate is verified in the literature (Kwon et al., 2014). In our MetS mouse model fed a high-fat diet rich in palmitate, switching to a diet that contains the same fat calories from oleate protects the peripheral nerves from palmitate-induced injury (Rumora et al., 2019). In epidemiological studies, plasma monounsaturated fatty acid levels inversely correlate with insulin resistance (Palomer et al., 2018), the MetS (Guo et al., 2017; Tortosa-Caparrós et al., 2017) and Alzheimer's disease (Solfrizzi et al., 2011; Beydoun et al., 2014). The differential effect of oleate versus palmitate on EV production is recapitulated in various cultures, including hepatocytes (Hirsova et al., 2016) and proximal tubular epithelial cells (Cobbs et al., 2019). Furthermore, EVs from palmitate-treated myotubes induce insulin resistance in recipient myotubes, whereas oleate-derived EVs do not (Aswad et al., 2014). A mechanistic study in hepatocytes proposed oleate does not enhance EV secretion because it is not a direct substrate for the formation of ceramides (Fukushima et al., 2018), which are implicated in EV biogenesis (Verderio et al., 2018) and Alzheimer's disease (Dinkins et al., 2017). Thus, our results suggest a possible molecular link between dietary oleate and diminished Alzheimer's disease risk via lower EV production.

We also investigated communication between oligodendrocytes and neurons via EVs. Oligodendrocytes primarily function in axon myelination in the brain to facilitate signal transmission. Insulin and insulin-like growth factor I (IGF-I) play important roles in myelin synthesis and maintenance and oligodendrocyte survival (Grote & Wright, 2016). Therefore, disrupted insulin and IGF-I signalling in MetS conditions elicits oligodendrocyte dysfunction and myelin loss, leading to white matter atrophy and degeneration, as frequently seen in Alzheimer's disease (Nasrabad et al., 2018). We found palmitate promoted insulin resistance in oligodendrocytes, which would interfere with their physiological function and support of neurons with implications for Alzheimer's disease onset and development.

Furthermore, brain metabolism occurs non-cell autonomously, involving communication between neurons and glia, including oligodendrocytes (Henn et al., 2022) through extracellular vesicles. Oligodendrocyte-derived EVs can exert either neurotoxic or neuroprotective effects, depending on the physiological conditions (Oyarce et al., 2022). Further, they support nutrient-deprived neurons, improving the metabolic state and promoting axonal transport (Fruhbeis et al., 2020). In our study, EVs from palmitate-treated oligodendrocytes could be transmitted to naïve recipient neurons, instigating insulin resistance. IRS-1 is aberrantly phosphorylated in neuronally-derived circulating EVs from Alzheimer's disease patients (Kapogiannis et al., 2015; Mullins et al., 2017). However, information specifically regarding neuron-oligodendrocyte communication via EVs on regulation of brain metabolism is lacking. Our findings shed light on the possible role of EVs in connecting insulin resistance in the brain with Alzheimer's disease, especially in the framework of glia-neuron interactions.

Despite molecular and epidemiological links, how MetS leads to Alzheimer's disease is not fully understood. As depicted on our model (Figure 7), the current results of neuron-neuron as well as oligodendrocyte-neuron interaction through insulin resistance-induced EVs provide a glimpse into how MetS conditions may spread Alzheimer's disease pathology in the brain. Our findings suggest a possible mechanism linking palmitate and glucose overconsumption and insulin resistance in the MetS with



increased risk of Alzheimer's disease. Additionally, it emphasises the important role of specific neuron-glia interaction during the MetS to further initiation of neuronal insulin resistance and eventual neurodegeneration.

## AUTHOR CONTRIBUTIONS

**Bhumsoo Kim:** Conceptualization; formal analysis; investigation; methodology; project administration; supervision; validation; visualization; writing—original draft; writing—review and editing. **Yoon-Tae Kang:** Investigation; methodology. **Faye E. Mendelson:** Investigation; writing—review and editing. **John M Hayes:** Investigation; methodology. **Masha G. Savellieff:** Visualization; writing—original draft; writing—review and editing. **Sunitha Nagrath:** Funding acquisition; supervision; writing—review and editing. **Eva L. Feldman:** Conceptualization; funding acquisition; project administration; supervision; writing—review and editing.

## ACKNOWLEDGEMENTS

The authors received funding support from the NIH (U24DK115255, R01DK130913). The authors would like to thank the Sinai Medical Staff Foundation, the Robert E. Niderlander Sr. Program for Alzheimer's Research, the Andrea and Lawrence A. Wolfe Brain Health Initiative Fund, the A. Alfred Taubman Medical Research Institute, and the NeuroNetwork for Emerging Therapies. The authors appreciate the support from the Michigan Diabetes Research Center for the confocal imaging.

## CONFLICT OF INTEREST STATEMENT

The authors declare they have no conflict of interest.

## ORCID

Bhumsoo Kim  <https://orcid.org/0000-0002-2645-1673>

## REFERENCES

- Ahn, J.-H., So, S.-P., Kim, N.-Y., Kim, H.-J., Yoon, S.-Y., & Kim, D.-H. (2016). c-Jun N-terminal Kinase (JNK) induces phosphorylation of amyloid precursor protein (APP) at Thr668, in okadaic acid-induced neurodegeneration. *BMB Reports*, *49*(7), 376–381.
- Akbar, N., Azzimato, V., Choudhury, R. P., & Aouadi, M. (2019). Extracellular vesicles in metabolic disease. *Diabetologia*, *62*(12), 2179–2187.
- Andrew, R. J., Kellett, K. A., Thinakaran, G., & Hooper, N. M. (2016). A Greek tragedy: The growing complexity of Alzheimer amyloid precursor protein proteolysis. *Journal of Biological Chemistry*, *291*(37), 19235–19244.
- Aswad, H., Forterre, A., Wiklander, O. P., Vial, G., Danty-Berger, E., Jalabert, A., Lamaziere, A., Meugnier, E., Pesenti, S., Ott, C., Chikh, K., El-Andaloussi, S., Vidal, H., Lefai, E., Rieusset, J., & Rome, S. (2014). Exosomes participate in the alteration of muscle homeostasis during lipid-induced insulin resistance in mice. *Diabetologia*, *57*(10), 2155–2164.
- Barron, A. M., Rosario, E. R., Elteriefi, R., & Pike, C. J. (2013). Sex-specific effects of high fat diet on indices of metabolic syndrome in 3xTg-AD mice: Implications for Alzheimer's disease. *PLoS ONE*, *8*(10), e78554–e78554.
- Beydoun, M. A., Beydoun, H. A., Gamaldo, A. A., Teel, A., Zonderman, A. B., & Wang, Y. (2014). Epidemiologic studies of modifiable factors associated with cognition and dementia: Systematic review and meta-analysis. *BMC Public Health [Electronic Resource]*, *14*, 643–643.
- Biessels, G. J., & Despa, F. (2018). Cognitive decline and dementia in diabetes mellitus: Mechanisms and clinical implications. *Nature Reviews Endocrinology*, *14*(10), 591–604.
- Busquets, O., Ettcheto, M., Pallas, M., Beas-Zarate, C., Verdaguer, E., Auladell, C., Folch, J., & Camins, A. (2017). Long-term exposition to a high fat diet favors the appearance of beta-amyloid depositions in the brain of C57BL/6J mice. A potential model of sporadic Alzheimer's disease. *Mechanisms of Ageing and Development*, *162*, 38–45.
- Campos-Pena, V., Toral-Rios, D., Becerril-Perez, F., Sanchez-Torres, C., Delgado-Namorado, Y., Torres-Ossorio, E., Franco-Bocanegra, D., & Carvajal, K. (2017). Metabolic syndrome as a risk factor for Alzheimer's disease: Is Abeta a crucial factor in both pathologies? *Antioxid Redox Signaling*, *26*(10), 542–560.
- Chen, J. F., Liu, K., Hu, B., Li, R. R., Xin, W., Chen, H., Wang, F., Chen, L., Li, R. X., Ren, S. Y., Xiao, L., Chan, J. R., & Mei, F. (2021). Enhancing myelin renewal reverses cognitive dysfunction in a murine model of Alzheimer's disease. *Neuron*, *109*(14), 2292–2307.e2295.
- Chen, W., Cai, W., Hoover, B., & Kahn, C. R. (2022). Insulin action in the brain: Cell types, circuits, and diseases. *Trends in Neuroscience (Tins)*, *45*(5), 384–400.
- Chen, Y., Li, J., Ma, B., Li, N., Wang, S., Sun, Z., Xue, C., Han, Q., Wei, J., & Zhao, R. C. (2020). MSC-derived exosomes promote recovery from traumatic brain injury via microglia/macrophages in rat. *Ageing (Albany NY)*, *12*(18), 18274–18296.
- Cobbs, A., Chen, X., Zhang, Y., George, J., Huang, M. B., Bond, V., Thompson, W., & Zhao, X. (2019). Saturated fatty acid stimulates production of extracellular vesicles by renal tubular epithelial cells. *Molecular and Cellular Biochemistry*, *458*(1-2), 113–124.
- Copps, K. D., & White, M. F. (2012). Regulation of insulin sensitivity by serine/threonine phosphorylation of insulin receptor substrate proteins IRS1 and IRS2. *Diabetologia*, *55*(10), 2565–2582.
- DeLeo, A. M., & Ikezu, T. (2018). Extracellular vesicle biology in Alzheimer's disease and related tauopathy. *Journal of Neuroimmune Pharmacology*, *13*(3), 292–308.
- Dinkins, M. B., Wang, G., & Bieberich, E. (2017). Sphingolipid-enriched extracellular vesicles and Alzheimer's disease: A decade of research. *Journal of Alzheimer's Disease*, *60*(3), 757–768.
- Eguchi, A., Lazić, M., Armando, A. M., Phillips, S. A., Katebian, R., Maraka, S., Quehenberger, O., Sears, D. D., & Feldstein, A. E. (2016). Circulating adipocyte-derived extracellular vesicles are novel markers of metabolic stress. *Journal of Molecular Medicine*, *94*(11), 1241–1253.
- Elzinga, S. E., Henn, R., Murdock, B. J., Kim, B., Hayes, J. M., Mendelson, F., Webber-Davis, I., Teener, S., Pacut, C., Lentz, S. I., & Feldman, E. L. (2022). cGAS/STING and innate brain inflammation following acute high-fat feeding. *Frontiers in Immunology*, *13*, 1012594.
- Freeman, D. W., Noren Hooten, N., Eitan, E., Green, J., Mode, N. A., Bodogai, M., Zhang, Y., Lehrmann, E., Zonderman, A. B., Biragyn, A., Egan, J., Becker, K. G., Mattson, M. P., Ejiogu, N., & Evans, M. K. (2018). Altered extracellular vesicle concentration, cargo, and function in diabetes. *Diabetes*, *67*(11), 2377–2388.

- Fruhbeis, C., Kuo-Elsner, W. P., Muller, C., Barth, K., Peris, L., Tenzer, S., Mobius, W., Werner, H. B., Nave, K. A., Frohlich, D., & Kramer-Albers, E. M. (2020). Oligodendrocytes support axonal transport and maintenance via exosome secretion. *PLoS Biology*, *18*(12), e3000621.
- Fukushima, M., Dasgupta, D., Mauer, A. S., Kakazu, E., Nakao, K., & Malhi, H. (2018). StAR-related lipid transfer domain II (STARDII)-mediated ceramide transport mediates extracellular vesicle biogenesis. *Journal of Biological Chemistry*, *293*(39), 15277–15289.
- Gasparini, L., Gouras, G. K., Wang, R., Gross, R. S., Beal, M. F., Greengard, P., & Xu, H. (2001). Stimulation of beta-amyloid precursor protein trafficking by insulin reduces intraneuronal beta-amyloid and requires mitogen-activated protein kinase signaling. *Journal of Neuroscience*, *21*(8), 2561–2570.
- Gerakis, Y., & Hetz, C. (2018). Emerging roles of ER stress in the etiology and pathogenesis of Alzheimer's disease. *The Febs Journal*, *285*(6), 995–1011.
- Grandl, G., & Wolfrum, C. (2018). Hemostasis, endothelial stress, inflammation, and the metabolic syndrome. *Seminars in Immunopathology*, *40*(2), 215–224.
- Grote, C. W., & Wright, D. E. (2016). A role for insulin in diabetic neuropathy. *Frontiers in Neuroscience*, *10*, 581.
- Grundy, S. M., Cleeman, J. I., Daniels, S. R., Donato, K. A., Eckel, R. H., Franklin, B. A., Gordon, D. J., Krauss, R. M., Savage, P. J., Smith, S. C., Jr., Spertus, J. A., & Costa, F. (2005). Diagnosis and management of the metabolic syndrome: An American Heart Association/National Heart, Lung, and Blood Institute Scientific Statement. *Circulation*, *112*(17), 2735–2752.
- Guo, X.-F., Li, X., Shi, M., & Li, D. (2017). n-3 Polyunsaturated fatty acids and metabolic syndrome risk: A meta-analysis. *Nutrients*, *9*(7), 703.
- Helwa, I., Cai, J., Drewry, M. D., Zimmerman, A., Dinkins, M. B., Khaled, M. L., Seremwe, M., Dismuke, W. M., Bieberich, E., Stamer, W. D., Hamrick, M. W., & Liu, Y. (2017). A comparative study of serum exosome isolation using differential ultracentrifugation and three commercial reagents. *PLoS ONE*, *12*(1), e0170628.
- Henn, R. E., Noureldein, M. H., Elzinga, S. E., Kim, B., Savelieff, M. G., & Feldman, E. L. (2022). Glial-neuron crosstalk in health and disease: A focus on metabolism, obesity, and cognitive impairment. *Neurobiology of Disease*, *170*, 105766.
- Hirsova, P., Ibrahim, S. H., Krishnan, A., Verma, V. K., Bronk, S. F., Werneburg, N. W., Charlton, M. R., Shah, V. H., Malhi, H., & Gores, G. J. (2016). Lipid-induced signaling causes release of inflammatory extracellular vesicles from hepatocytes. *Gastroenterology*, *150*(4), 956–967.
- Johe, K. K., Hazel, T. G., Muller, T., Dugich-Djordjevic, M. M., & McKay, R. D. (1996). Single factors direct the differentiation of stem cells from the fetal and adult central nervous system. *Genes & Development*, *10*(24), 3129–3140.
- Kapogiannis, D., Boxer, A., Schwartz, J. B., Abner, E. L., Biragyn, A., Masharani, U., Frassetto, L., Petersen, R. C., Miller, B. L., & Goetzl, E. J. (2015). Dysfunctionally phosphorylated type 1 insulin receptor substrate in neural-derived blood exosomes of preclinical Alzheimer's disease. *FASEB Journal*, *29*(2), 589–596.
- Kellar, D., & Craft, S. (2020). Brain insulin resistance in Alzheimer's disease and related disorders: Mechanisms and therapeutic approaches. *Lancet Neurology*, *19*(9), 758–766.
- Kim, B., Backus, C., Oh, S., & Feldman, E. L. (2013). Hyperglycemia-induced tau cleavage in vitro and in vivo: A possible link between diabetes and Alzheimer's disease. *Journal of Alzheimer's Disease*, *34*(3), 727–739.
- Kim, B., Backus, C., Oh, S., Hayes, J. M., & Feldman, E. L. (2009). Increased tau phosphorylation and cleavage in mouse models of type 1 and type 2 diabetes. *Endocrinology*, *150*(12), 5294–5301.
- Kim, B., Elzinga, S. E., Henn, R. E., McGinley, L. M., & Feldman, E. L. (2019). The effects of insulin and insulin-like growth factor I on amyloid precursor protein phosphorylation in in vitro and in vivo models of Alzheimer's disease. *Neurobiology of Disease*, *132*, 104541.
- Kim, B., & Feldman, E. L. (2012). Insulin resistance in the nervous system. *Trends in Endocrinology and Metabolism*, *23*(3), 133–141.
- Kim, B., & Feldman, E. L. (2015). Insulin resistance as a key link for the increased risk of cognitive impairment in the metabolic syndrome. *Experimental & Molecular Medicine*, *47*, e149.
- Kim, B., Figueroa-Romero, C., Pacut, C., Backus, C., & Feldman, E. L. (2015). Insulin resistance prevents AMPK-induced tau dephosphorylation through Akt-mediated increase in AMPKSer-485 phosphorylation. *Journal of Biological Chemistry*, *290*(31), 19146–19157.
- Kim, B., McLean, L. L., Philip, S. S., & Feldman, E. L. (2011). Hyperinsulinemia induces insulin resistance in dorsal root ganglion neurons. *Endocrinology*, *152*(10), 3638–3647.
- Kim, B., Sullivan, K. A., Backus, C., & Feldman, E. L. (2011). Cortical neurons develop insulin resistance and blunted Akt signaling: A potential mechanism contributing to enhanced ischemic injury in diabetes. *Antioxid Redox Signaling*, *14*(10), 1829–1839.
- Kim, J., Park, Y. J., Jang, Y., & Kwon, Y. H. (2011). AMPK activation inhibits apoptosis and tau hyperphosphorylation mediated by palmitate in SH-SY5Y cells. *Brain Research*, *1418*, 42–51.
- Kowal, J., Arras, G., Colombo, M., Jouve, M., Morath, J. P., Primdal-Bengtson, B., Dingli, F., Loew, D., Tkach, M., & Thery, C. (2016). Proteomic comparison defines novel markers to characterize heterogeneous populations of extracellular vesicle subtypes. *PNAS*, *113*(8), E968–E977.
- Kwon, B., Lee, H.-K., & Querfurth, H. W. (2014). Oleate prevents palmitate-induced mitochondrial dysfunction, insulin resistance and inflammatory signaling in neuronal cells. *Biochimica et Biophysica Acta*, *1843*(7), 1402–1413.
- Laulagnier, K., Javelot, C., Hemming, F. J., Chivet, M., Lachenal, G., Blot, B., Chatellard, C., & Sadoul, R. (2018). Amyloid precursor protein products concentrate in a subset of exosomes specifically endocytosed by neurons. *Cellular and Molecular Life Sciences*, *75*(4), 757–773.
- Lee, M. S., Kao, S. C., Lemere, C. A., Xia, W., Tseng, H. C., Zhou, Y., Neve, R., Ahljian, M. K., & Tsai, L. H. (2003). APP processing is regulated by cytoplasmic phosphorylation. *Journal of Cell Biology*, *163*(1), 83–95.
- Lombino, F., Biundo, F., Tamayev, R., Arancio, O., & D'Adamio, L. (2013). An intracellular threonine of amyloid-beta precursor protein mediates synaptic plasticity deficits and memory loss. *PLoS ONE*, *8*(2), e57120.
- Marco, D. Y. L., Venneri, A., Farkas, E., Evans, P. C., Marzo, A., & Frangi, A. F. (2015). Vascular dysfunction in the pathogenesis of Alzheimer's disease—A review of endothelium-mediated mechanisms and ensuing vicious circles. *Neurobiology of Disease*, *82*, 593–606.
- Martinez, M. C., & Andriantsitohaina, R. (2017). Extracellular vesicles in metabolic syndrome. *Circulation Research*, *120*(10), 1674–1686.
- Marwarha, G., Claycombe-Larson, K., Lund, J., Schommer, J., & Ghribi, O. (2019). A diet enriched in palmitate and deficient in linoleate exacerbates oxidative stress and amyloid-beta burden in the hippocampus of 3xTg-AD mouse model of Alzheimer's disease. *Journal of Alzheimer's Disease*, *68*(1), 219–237.
- Marwarha, G., Rostad, S., Lilek, J., Kleinjan, M., Schommer, J., & Ghribi, O. (2017). Palmitate increases beta-site AbetaPP-cleavage enzyme 1 activity and amyloid-beta genesis by evoking endoplasmic reticulum stress and subsequent C/EBP homologous protein activation. *Journal of Alzheimer's Disease*, *57*(3), 907–925.
- Matioli, M., & Nitrini, R. (2015). Mechanisms linking brain insulin resistance to Alzheimer's disease. *Dementia & Neuropsychologia*, *9*(2), 96–102.
- Matsushima, T., Saito, Y., Elliott, J. I., Iijima-Ando, K., Nishimura, M., Kimura, N., Hata, S., Yamamoto, T., Nakaya, T., & Suzuki, T. (2012). Membrane-microdomain localization of amyloid beta-precursor protein (APP) C-terminal fragments is regulated by phosphorylation of the cytoplasmic Thr668 residue. *Journal of Biological Chemistry*, *287*(23), 19715–19724.
- Miranda, A. M., Lasiecka, Z. M., Xu, Y., Neufeld, J., Shahriar, S., Simoes, S., Chan, R. B., Oliveira, T. G., Small, S. A., & Di Paolo, G. (2018). Neuronal lysosomal dysfunction releases exosomes harboring APP C-terminal fragments and unique lipid signatures. *Nature Communications*, *9*(1), 291.
- Mohan, S., R. P. R. M., Brown, L., Ayyappan, P., & R. K. G. (2019). Endoplasmic reticulum stress: A master regulator of metabolic syndrome. *European Journal of Pharmacology*, *860*, 172553.

- Mullins, R. J., Mustapic, M., Goetzl, E. J., & Kapogiannis, D. (2017). Exosomal biomarkers of brain insulin resistance associated with regional atrophy in Alzheimer's disease. *Human Brain Mapping, 38*(4), 1933–1940.
- Nakandakari, S., Muñoz, V. R., Kuga, G. K., Gaspar, R. C., Sant'Ana, M. R., Pavan, I. C. B., da Silva, L. G. S., Morelli, A. P., Simabuco, F. M., da Silva, A. S. R., de Moura, L. P., Ropelle, E. R., Cintra, D. E., & Pauli, J. R. (2019). Short-term high-fat diet modulates several inflammatory, ER stress, and apoptosis markers in the hippocampus of young mice. *Brain, Behavior, and Immunity, 79*, 284–293.
- Nasrabady, S. E., Rizvi, B., Goldman, J. E., & Brickman, A. M. (2018). White matter changes in Alzheimer's disease: A focus on myelin and oligodendrocytes. *Acta Neuropathologica Communications, 6*(1), 22.
- Neth, B. J., & Craft, S. (2017). Insulin resistance and Alzheimer's disease: Bioenergetic linkages. *Frontiers in Aging Neuroscience, 9*, 345.
- O'Grady, J. P., Dean, D. C. 3rd, Yang, K. L., Canda, C. M., Hoscheidt, S. M., Starks, E. J., Merluzzi, A., Hurley, S., Davenport, N. J., Okonkwo, O. C., Anderson, R. M., Asthana, S., Johnson, S. C., Alexander, A. L., & Bendlin, B. B. (2019). Elevated insulin and insulin resistance are associated with altered myelin in cognitively unimpaired middle-aged adults. *Obesity (Silver Spring), 27*(9), 1464–1471.
- O'Neill, S., & O'Driscoll, L. (2015). Metabolic syndrome: A closer look at the growing epidemic and its associated pathologies. *Obesity Reviews, 16*(1), 1–12.
- Ono, H. (2019). Molecular mechanisms of hypothalamic insulin resistance. *International Journal of Molecular Sciences, 20*(6), 1317.
- Oyarce, K., Cepeda, M. Y., Lagos, R., Garrido, C., Vega-Letter, A. M., Garcia-Robles, M., Luz-Crawford, P., & Elizondo-Vega, R. (2022). Neuroprotective and neurotoxic effects of glial-derived exosomes. *Frontiers in Cellular Neuroscience, 16*, 920686.
- Palomer, X., Pizarro-Delgado, J., Barroso, E., & Vazquez-Carrera, M. (2018). Palmitic and oleic acid: The Yin and Yang of fatty acids in type 2 diabetes mellitus. *Trends in Endocrinology and Metabolism, 29*(3), 178–190.
- Pardini, G., Pace, V., Copani, A., Squatrito, S., Milardi, D., & Vigneri, R. (2013). Insulin has multiple anti-amyloidogenic effects on human neuronal cells. *Endocrinology, 154*(1), 375–387.
- Pardo, F., Villalobos-Labra, R., Sobrevia, B., Toledo, F., & Sobrevia, L. (2018). Extracellular vesicles in obesity and diabetes mellitus. *Molecular Aspects of Medicine, 60*, 81–91.
- Patil, S., Sheng, L., Masserang, A., & Chan, C. (2006). Palmitic acid-treated astrocytes induce BACE1 upregulation and accumulation of C-terminal fragment of APP in primary cortical neurons. *Neuroscience Letters, 406*(1–2), 55–59.
- Pedditz, E., Peters, R., & Beckett, N. (2016). The risk of overweight/obesity in mid-life and late life for the development of dementia: A systematic review and meta-analysis of longitudinal studies. *Age and Ageing, 45*(1), 14–21.
- Perez-Gonzalez, R., Kim, Y., Miller, C., Pacheco-Quinto, J., Eckman, E. A., & Levy, E. (2020). Extracellular vesicles: Where the amyloid precursor protein carboxyl-terminal fragments accumulate and amyloid-beta oligomerizes. *FASEB Journal, 34*(9), 12922–12931.
- Power, M. C., Rawlings, A. A. R., Bandeen-Roche, K., Coresh, J., Ballantyne, C. M., Pokharel, Y., Michos, E. D., Penman, A., Alonso, A., Knopman, D., Mosley, T. H., & Gottesman, R. F. (2018). Association of midlife lipids with 20-year cognitive change: A cohort study. *Alzheimers Dement, 14*(2), 167–177.
- Ramelot, T. A., & Nicholson, L. K. (2001). Phosphorylation-induced structural changes in the amyloid precursor protein cytoplasmic tail detected by NMR. *Journal of Molecular Biology, 307*(3), 871–884.
- Rollins, C. P. E., Gallino, D., Kong, V., Ayranci, G., Devenyi, G. A., Germann, J., & Chakravarty, M. M. (2019). Contributions of a high-fat diet to Alzheimer's disease-related decline: A longitudinal behavioural and structural neuroimaging study in mouse models. *NeuroImage: Clinical, 21*, 101606.
- Rumora, A. E., Lentz, S. I., Hinder, L. M., Jackson, S. W., Valesano, A., Levinson, G. E., & Feldman, E. L. (2018). Dyslipidemia impairs mitochondrial trafficking and function in sensory neurons. *FASEB Journal, 32*(1), 195–207.
- Rumora, A. E., LoGrasso, G., Hayes, J. M., Mendelson, F. E., Tabbey, M. A., Haidar, J. A., Lentz, S. I., & Feldman, E. L. (2019). The divergent roles of dietary saturated and monounsaturated fatty acids on nerve function in murine models of obesity. *Journal of Neuroscience, 39*(19), 3770–3781.
- Sadahiro, R., Sawada, N., Matsuoka, Y. J., Mimura, M., Nozaki, S., Shikimoto, R., Goto, A., & Tsugane, S. (2019). Midlife cancer/diabetes and risk of dementia and mild cognitive impairment: A population-based prospective cohort study in Japan. *Psychiatry and Clinical Neurosciences, 73*(9), 597–599.
- Sardar Sinha, M., Ansell-Schultz, A., Civitelli, L., Hildesjo, C., Larsson, M., Lannfelt, L., Ingelsson, M., & Hallbeck, M. (2018). Alzheimer's disease pathology propagation by exosomes containing toxic amyloid-beta oligomers. *Acta Neuropathologica, 136*(1), 41–56.
- Savelieff, M. G., Lee, S., Liu, Y., & Lim, M. H. (2013). Untangling amyloid- $\beta$ , tau, and metals in Alzheimer's disease. *ACS Chemical Biology, 8*(5), 856–865.
- Sims-Robinson, C., Kim, B., Rosko, A., & Feldman, E. L. (2010). How does diabetes accelerate Alzheimer disease pathology? *Nature Reviews Neuroscience England, 6*, 551–559.
- Solfrizzi, V., Panza, F., Frisardi, V., Seripa, D., Logroscino, G., Imbimbo, B. P., & Pilotto, A. (2011). Diet and Alzheimer's disease risk factors or prevention: The current evidence. *Expert Review of Neurotherapeutics, 11*(5), 677–708.
- Soo, C. Y., Song, Y., Zheng, Y., Campbell, E. C., Riches, A. C., Gunn-Moore, F., & Powis, S. J. (2012). Nanoparticle tracking analysis monitors microvesicle and exosome secretion from immune cells. *Immunology, 136*(2), 192–197.
- Standen, C. L., Brownlees, J., Grierson, A. J., Kesavapany, S., Lau, K. F., McLoughlin, D. M., & Miller, C. C. (2001). Phosphorylation of thr(668) in the cytoplasmic domain of the Alzheimer's disease amyloid precursor protein by stress-activated protein kinase 1b (Jun N-terminal kinase-3). *Journal of Neurochemistry, 76*(1), 316–320.
- Takeda, S., Sato, N., Uchio-Yamada, K., Sawada, K., Kunieda, T., Takeuchi, D., Kurinami, H., Shinohara, M., Rakugi, H., & Morishita, R. (2010). Diabetes-accelerated memory dysfunction via cerebrovascular inflammation and A $\beta$  deposition in an Alzheimer mouse model with diabetes. *PNAS, 107*(15), 7036–7041.
- Thery, C., Witwer, K. W., Aikawa, E., Alcaraz, M. J., Anderson, J. D., Andriantsitohaina, R., Antoniou, A., Arab, T., Archer, F., Atkin-Smith, G. K., Ayre, D. C., Bach, J. M., Bachurski, D., Baharvand, H., Balaj, L., Baldacchino, S., Bauer, N. N., Baxter, A. A., Bebawy, M., ... Zuba-Surma, E. K. (2018). Minimal information for studies of extracellular vesicles 2018 (MISEV2018): A position statement of the International Society for Extracellular Vesicles and update of the MISEV2014 guidelines. *J Extracell Vesicles, 7*(1), 1535750.
- Tortosa-Caparrós, E., Navas-Carrillo, D., Marín, F., & Orenes-Piñero, E. (2017). Anti-inflammatory effects of omega 3 and omega 6 polyunsaturated fatty acids in cardiovascular disease and metabolic syndrome. *Critical Reviews in Food Science and Nutrition, 57*(16), 3421–3429.
- Van Dyken, P., & Lacoste, B. (2018). Impact of metabolic syndrome on neuroinflammation and the blood-brain barrier. *Frontiers in Neuroscience, 12*, 930.
- van Niel, G., D'Angelo, G., & Raposo, G. (2018). Shedding light on the cell biology of extracellular vesicles. *Nature Reviews Molecular Cell Biology, 19*(4), 213–228.
- Vanzulli, I., Papanikolaou, M., De-La-Rocha, I. C., Pieropan, F., Rivera, A. D., Gomez-Nicola, D., Verkhatsky, A., Rodriguez, J. J., & Butt, A. M. (2020). Disruption of oligodendrocyte progenitor cells is an early sign of pathology in the triple transgenic mouse model of Alzheimer's disease. *Neurobiology of Aging, 94*, 130–139.
- Vella, L. J., Scicluna, B. J., Cheng, L., Bawden, E. G., Masters, C. L., Ang, C. S., Williamson, N., McLean, C., Barnham, K. J., & Hill, A. F. (2017). A rigorous method to enrich for exosomes from brain tissue. *Journal of Extracellular Vesicles, 6*(1), 1348885.
- Verderio, C., Gabrielli, M., & Giussani, P. (2018). Role of sphingolipids in the biogenesis and biological activity of extracellular vesicles. *Journal of Lipid Research, 59*(8), 1325–1340.

- Verdile, G., Keane, K. N., Cruzat, V. F., Medic, S., Sabale, M., Rowles, J., Wijesekara, N., Martins, R. N., Fraser, P. E., & Newsholme, P. (2015). Inflammation and oxidative stress: The molecular connectivity between insulin resistance, obesity, and Alzheimer's disease. *Mediators of Inflammation*, 2015, 105828.
- Vincent, A. M., McLean, L. L., Backus, C., & Feldman, E. L. (2005). Short-term hyperglycemia produces oxidative damage and apoptosis in neurons. *FASEB Journal*, 19(6), 638–640.
- Vingtdeux, V., Hamdane, M., Gompel, M., Begard, S., Drobecq, H., Ghestem, A., Grosjean, M. E., Kostanjevecki, V., Grognet, P., Vanmechelen, E., Buee, L., Delacourte, A., & Sergeant, N. (2005). Phosphorylation of amyloid precursor carboxy-terminal fragments enhances their processing by a gamma-secretase-dependent mechanism. *Neurobiology of Disease*, 20(2), 625–637.
- Vinuesa, A., Bentivegna, M., Calfa, G., Filipello, F., Pomilio, C., Bonaventura, M. M., Lux-Lantos, V., Matzkin, M. E., Gregosa, A., Presa, J., Matteoli, M., Beauquis, J., & Saravia, F. (2019). Early exposure to a high-fat diet impacts on hippocampal plasticity: Implication of microglia-derived exosome-like extracellular vesicles. *Molecular Neurobiology*, 56(7), 5075–5094.
- Wang, Y., Balaji, V., Kaniyappan, S., Kruger, L., Irsen, S., Tepper, K., Chandupatla, R., Maetzler, W., Schneider, A., Mandelkow, E., & Mandelkow, E. M. (2017). The release and trans-synaptic transmission of Tau via exosomes. *Molecular Neurodegeneration*, 12(1), 5.
- Winston, C. N., Goetzl, E. J., Akers, J. C., Carter, B. S., Rockenstein, E. M., Galasko, D., Masliah, E., & Rissman, R. A. (2016). Prediction of conversion from mild cognitive impairment to dementia with neuronally derived blood exosome protein profile. *Alzheimer's & Dementia (Amsterdam, Netherlands)*, 3, 63–72.
- Xiao, T., Zhang, W., Jiao, B., Pan, C. Z., Liu, X., & Shen, L. (2017). The role of exosomes in the pathogenesis of Alzheimer's disease. *Translational Neurodegeneration*, 6, 3.
- Yarza, R., Vela, S., Solas, M., & Ramirez, M. J. (2015). c-Jun N-terminal Kinase (JNK) signaling as a therapeutic target for Alzheimer's disease. *Frontiers in Pharmacology*, 6, 321.

## SUPPORTING INFORMATION

Additional supporting information can be found online in the Supporting Information section at the end of this article.

**How to cite this article:** Kim, B., Kang, Y.-T., Mendelson, F. E., Hayes, J. M., Savelieff, M. G., Nagrath, S., & Feldman, E. L. (2023). Palmitate and glucose increase amyloid precursor protein in extracellular vesicles: Missing link between metabolic syndrome and Alzheimer's disease. *Journal of Extracellular Vesicles*, 12, e12340.  
<https://doi.org/10.1002/jev2.12340>